Three-Dimensional Data on Limb Extremities of Ungulates with Pads Provide Insights into Morphological Changes Associated with the Evolution of Unguligrady

Authors: Takeda, Sei-ichiro, Nguyen, Truong Son, and Endo, Hideki

Source: Mammal Study, 50(3) : 1-10

Published By: Mammal Society of Japan

URL: https://doi.org/10.3106/ms2024-0013

Mammal Study 50 (2025) DOI: 10.3106/ms2024-0013

Original paper

Three-dimensional data on limb extremities of ungulates with pads provide insights into morphological changes associated with the evolution of unguligrady

Sei-ichiro Takeda[1,2,*], Truong Son Nguyen[3,4] and Hideki Endo[1]

[1] *The University Museum, The University of Tokyo 7-3-1 Hongo, Bunkyo-ku, Tokyo 113-0032, Japan*
[2] *Graduate School of Agricultural and Life Sciences, The University of Tokyo, 1-1-1, Yayoi, Bunkyo-ku, Tokyo 113-0032, Japan*
[3] *Department of Zoology, Institute of Ecology and Biological Resources, Vietnam Academy of Sciences and Technology, Hanoi 10072, Vietnam*
[4] *Graduate University of Science and Technology, Vietnam Academy of Science and Technology, Hanoi 11307, Vietnam*

Abstract. Camelidae and Hippopotamidae (Artiodactyla) and Rhinocerotidae and Tapiridae (Perissodactyla) are unguligrades with pads, which support their body weight with their hooves and volar pads on their feet. In order to investigate the evolution of unguligrady from a functional morphological point of view, it is necessary to examine the limbs of living unguligrades with pads. In this study, we focused on the extremities of limbs of camelids and rhinoceroses and analyzed the differences between them and those of bovids, which are unguligrade without pads, using CT to simulate three-dimensional movements. The results showed that metapodials and proximal phalanges were interlocked by pulleys in unguligrades, whereas a large gap was observed between metapodials and proximal phalanges in unguligrades with pads. However, the angle changes of proximal phalanges of unguligrades with pads were smaller than those observed in unguligrades. This suggests that the pads inhibit wide spreading of the digits in these taxa. Whereas unguligrades, such as bovids, have adapted to various terrains by modifying the mobility of their digits, our results suggest that volar pads have limited the ability of unguligrades with pads to adapt to a variety of terrains.

Key words: Artiodactyla, Camelidae, hooves, limbs, Perissodactyla.

Among ungulates, two types are distinguished as follows: 1) unguligrades, in which only the hoof contacts the ground, and 2) unguligrades that contact the ground with their hooves and pads composed of adipose and collagen fibers. Camelidae and Hippopotamidae (Artiodactyla) and Rhinocerotidae and Tapiridae (Perissodactyla) are the taxonomic groups with pads on the extremities of their limbs (Thomason 1986; Smuts and Bezuidenhout 1987; von Houwald 2001; Wilson and Mittermeier 2011). The fossil records suggest that both artiodactyls and perissodactyls evolved from digitigrades to unguligrades through unguligrades with pads (Clifford 2010). Hippopotamidae, Rhinocerotidae, and Tapiridae are equipped with the extremities of the padded stage in the unguligrade evolution, and are referred to as subunguligrades (Thomason 1986; Clifford 2010). Camelidae are classified as secondary digitigrade since they acquired unguligrade and then gained pads on the extremities of their limbs (Clifford 2010). In this study, both subungulidrade and secondary digitigrade were referred to as "unguligrade with pads" since they both share the morphological feature of possessing pads on the extremities of their limbs.

The function of the pads is to absorb shock and disperse foot pressure (Panagiotopoulou et al. 2012, 2016, 2019; Clemente et al. 2020) and thus contributes to the larger body size of unguligrades with pads. The advantage of unguligrady is an increase in running velocity due to the reduced weight of the extremities of limb (Gregory 1912; Howell 1944; Janis and Wilhelm 1993). Considering the difference between the advantages of unguligrade and unguligrade with pads, we would expect movements of extremity to be different in unguligrades and unguligrades with pads.

In this study, we examined the differences in locomo-

*To whom correspondence should be addressed. E-mail: se1rotakeda@gmail.com

tion of extremity between unguligrades and unguligrades with pads by comparing the morphology of extremities of limb. The angle between the proximal phalanges in opening and closing states varies in bovids (unguligrades) depending on the habitat (Takeda et al. 2023). Therefore, we focused on the angle of digit opening and closing in both unguligrades and unguligrades with pads to clarify whether the latter has the potential to adapt to diverse environments as the former.

Materials and methods

Necropsy specimens of *Camelus bactrianus*, *C. dromedarius*, *Capra falconeri*, *Ceratotherium simum*, *Hippopotamus amphibius*, *Lama glama*, *Oryx leucoryx*, *Ovis canadensis*, *Pseudois nayaur*, *Rhinoceros unicornis*, and *Tapirus indicus* that had been donated to The University Museum, The University of Tokyo (UMUT) were used (Table 1). All specimens were obtained in adherence to appropriate ethical standards. The institutions that donated the specimens are listed in Table 1. *Camelus bactrianus*, *C. dromedarius*, *L. glama*, *H. amphibius*, *C. simum*, *R. unicornis*, and *T. indicus* possess pads at extremities of limb, whereas *C. falconeri*, *O. leucoryx*, *O. canadensis*, and *P. nayaur* were unguligrades (Wilson and Mittermeier 2011).

We performed CT scanning and angle measurement methods from 3D images. A CT scanner (Asteion PREMIUM 4 EDITION, Toshiba Medical Systems, Tokyo, Japan) was used to serially section the extremities of the limbs from the parallel distal to the proximal planes at a 0.5 mm thickness, without a gap. The current and voltage were 100 mA and 120 kV, respectively (Endo et al. 2019; Takeda et al. 2023). The left forefoot and hindfoot were scanned in *C. bactrianus*, *C. dromedarius*, *L. glama*, *C. simum*, *R. unicornis*, *C. falconeri*, *O. leucoryx*, *O. canadensis*, and *P. nayaur*. The right forefoot and hindfoot were scanned in *C. simum* since the pads of the left forefoot and hindfoot had already been dissected at donation. The phalanges were positioned to simulate the opening and closing movements during CT scanning. During the opening state, the phalanges were opened to their furthest extent, whereas the phalanges and metacarpals or metatarsals were closed to their closest extent during the closing state. The obtained series of CT images were then used to reconstruct 3D images of the forefoot and hindfoot. First, we checked the 3D data of the skeleton for the presence of gaps at the metapodiophalangeal joint. Sagittal sections of the metapodiophalangeal joint were captured along the sagittal crest at the distal end of the metapodials. The images were used to measure the distances between the central distal end of the metapodials and the central proximal end of the proximal phalanges. The distances were examined using a 3D image analyzing system (Amira 2021.1: Visage Imaging GmbH, Berlin, Germany). For interspecies comparison of metapodiophalangeal joint gaps, the common logarithm of measured distances were divided by the common loga-

Table 1. Species used in this study

Order	Family	Species	Common name	Collection number	Institution	Posture
Artiodactyla	Bovidae	*Capra falconeri*	markhor	UMUT-21284	Yumemi Zoo	unguligrade
		Oryx leucoryx	Arabian oryx	UNUT-20196	Kanazawa Zoological Gardens	unguligrade
		Ovis canadensis	bighorn sheep	UMUT-20219	Kanazawa Zoological Gardens	unguligrade
		Pseudois nayaur	bharal	UMUT-20197	Kanazawa Zoological Gardens	unguligrade
	Camelidae	*Camelus bactorianus*	Bactrian camel	UMUT-21311	Tobu zoo	secondarily digitigrade
		Camelus dromerarius	dromedary camel	UMUT-22035	ZOORASIA	secondarily digitigrade
		Lama glama	llama	UMUT-23426	Izu Shaboten Zoo	secondarily digitigrade
	Hippopotamidae	*Hippopotamus amphibius*	hippopotamus	UMUT-17261	Kamine Zoo	subunguligrade
Perissodactyla	Tapiridae	*Tapirus indicus*	Malayan tapir	UMUT-22099	ZOORASIA	subunguligrade
	Rhinocerotidae	*Ceratotherium simum*	white rhinoceros	UMUT-21168	Tobu zoo	subunguligrade
		Rhinoceros unicornis	Indian rhinoceros	UMUT-22112	Kanazawa Zoological Gardens	subunguligrade

Unguligrades with pads are colored gray.

rithm of body mass in kg to the power of one-third and corrected for body size. The body masses referred to the weight of the specimens at the time of death. We ran Mann-Whitney U-tests to determine significant differences in the size of the gap between unguligrades and unguligrades with pads. Second, to quantify the opening and closing movements of the foot bones, the angle between the proximal phalanges was measured using a 3D image analysis software. We measured the angle between the third and fourth proximal phalanges in artiodactyls. In Perissodactyla (Rhinocerotidae), the angles between the second and third proximal phalanges and those between the third and fourth were measured. The angle of the phalanges was also examined using the 3D image analyzing system to quantitatively clarify the opening and closing movements of the foot bones. Landmarks were placed proximally and distally on the proximal phalanges. The three-dimensional coordinates of the landmarks were used to calculate the vector of each of the proximal phalanges. The angles were derived from the formula

$$\cos\theta = \frac{\vec{a} \cdot \vec{b}}{|\vec{a}||\vec{b}|}$$

using the vectors of the proximal phalanges. The angles between phalanges in the opening and closing states were measured, and the difference between the two angles was recorded. The landmarks used to measure angles and those in the reconstructed images are shown in Fig. 1.

Hippopotamuses and tapirs (both unguligrade with pads) were described as to digit mobility (Endo et al. 2019). The digit mobility of the camelidae and rhinocerotidae used in this study was compared with that of the hippopotamuses and the tapirs. We used the necropsy specimens of *C. dromedarius*, *R. unicornis*, *H. amphibius*, and *T. indicus* for the digit mobility comparisons. For these four species, we made macroscopic observations of the external morphology of the surface of the pads and described the differences in characteristics between species.

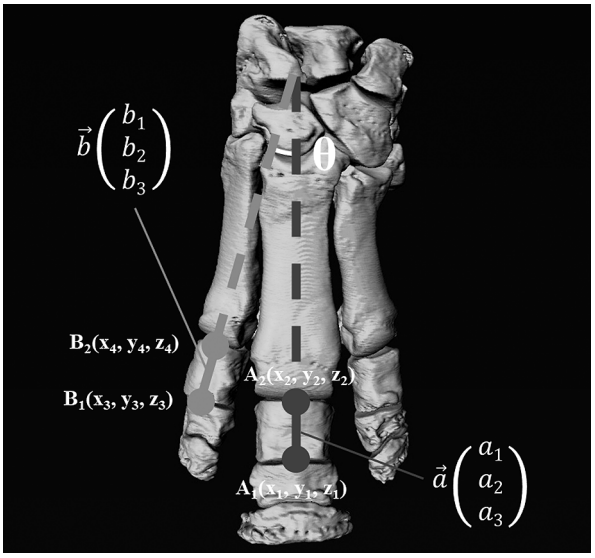

Fig. 1. Method of measuring angles (extremity of the left forelimb of *R. unicornis* viewed from dorsal aspect). Landmarks A_1 and A_2 were placed at the distal and proximal ends of the proximal phalanx with the 3D image analyzing system, and the coordinates of each point were obtained. From the coordinates, the vector ($\vec{a}$) of the proximal phalanx was calculated. This calculation was also performed for the other proximal phalanx and $\vec{b}$ was obtained. Using these two vectors, θ was calculated.

Results

Skeletal arrangement

In unguligrades (*C. falconeri*, *O. leucoryx*, *O. canadensis*, and *P. nayaur*), metapodials and proximal phalanges were interlocked by pulleys and no apparent gap was observed in the metapodiophalangeal joints (Tables 2 and 3; Fig. 2). In contrast, in the metapodiophalangeal joints of unguligrade with pads (*C. bactrianus*, *C. dromedarius*, *L. glama*, *C. simum*, and *R. unicornis*), large gaps were observed as the metapodials and proximal phalanges were not in direct contact (Tables 2 and 3; Figs. 3–7). Llamas inhabit mountainous terrain, whereas the other four species live in plains or wetlands (Wilson and Mittermeier 2011). Therefore, it was predicted that the metapodiophalangeal joints of *L. glama* would differ from those of the other four species. However, the gaps in the metapodiophalangeal joints of *L. glama* were the similar size as those of other four species. The Mann-Whitney U-tests showed that the gaps were significantly larger in unguligrades with pads at both metacarpophalangeal and metatarsophalangeal joints ($P < 0.001$ for both).

Angle

In the forelimb, angular differences between the opening and closing states of unguligrade species *C. falconeri*, *O. leucoryx*, *O. canadensis*, and *P. nayaur* were 7.5°, 2.2°, 6.3°, and 6.2°, respectively. Camelids (*C. bactrianus*, *C. dromedarius*, and *L. glama*) changed the angle of the proximal phalanges by 0.7°, 2.7°, and 5.4° between opening and closing, respectively (Table 4). In *C. simum* and *R. unicornis*, the angle changes of the proximal phalanges

Table 2. Gap size in the metacarpophalangeal joints

Species	Position	Gap size (mm)	Mass (kg)	{log(Gap size)}/{log($\sqrt[3]{mass}$)}
Capra falconeri	third metacarpophalangeal joint	1.05	106	0.031
	fourth metacarpophalangeal joint	1.04		0.025
Oryx leucoryx	third metacarpophalangeal joint	0.55	70	–0.422
	fourth metacarpophalangeal joint	0.67		–0.283
Ovis canadensis	third metacarpophalangeal joint	0.65	65	–0.310
	fourth metacarpophalangeal joint	0.91		–0.068
Pseudois nayaur	third metacarpophalangeal joint	0.47	62	–0.549
	fourth metacarpophalangeal joint	0.60		–0.371
Camelus bactorianus	third metacarpophalangeal joint	2.71	450	0.490
	fourth metacarpophalangeal joint	2.76		0.499
Camelus dromerarius	third metacarpophalangeal joint	2.14	681	0.350
	fourth metacarpophalangeal joint	2.96		0.499
Lama glama	third metacarpophalangeal joint	1.78	133	0.354
	fourth metacarpophalangeal joint	1.85		0.377
Ceratotherium simum	second metacarpophalangeal joint	4.16	2300	0.552
	third metacarpophalangeal joint	5.77		0.679
	fourth metacarpophalangeal joint	4.40		0.574
Rhinoceros unicornis	second metacarpophalangeal joint	3.05	2000	0.440
	third metacarpophalangeal joint	4.18		0.565
	fourth metacarpophalangeal joint	6.01		0.708

Backgrounds for unguligrades with pads are colored gray.

Table 3. Gap size in the metatarsophalangeal joints

Species	Position	Gap size (mm)	Mass (kg)	{log(Gap size)}/{log($\sqrt[3]{mass}$)}
Capra falconeri	third metatarsophalangeal joint	0.98	106	–0.013
	fourth metatarsophalangeal joint	1.04		0.025
Oryx leucoryx	third metatarsophalangeal joint	0.65	70	–0.304
	fourth metatarsophalangeal joint	0.50		–0.489
Ovis canadensis	third metatarsophalangeal joint	0.72	65	–0.236
	fourth metatarsophalangeal joint	0.68		–0.277
Pseudois nayaur	third metatarsophalangeal joint	0.55	62	–0.435
	fourth metatarsophalangeal joint	0.61		–0.359
Camelus bactorianus	third metatarsophalangeal joint	4.28	450	0.714
	fourth metatarsophalangeal joint	4.03		0.684
Camelus dromerarius	third metatarsophalangeal joint	2.43	681	0.408
	fourth metatarsophalangeal joint	2.19		0.360
Lama glama	third metatarsophalangeal joint	1.66	133	0.311
	fourth metatarsophalangeal joint	1.68		0.318
Ceratotherium simum	second metatarsophalangeal joint	3.17	2300	0.447
	third metatarsophalangeal joint	3.42		0.477
	fourth metatarsophalangeal joint	3.02		0.428
Rhinoceros unicornis	second metatarsophalangeal joint	2.44	2000	0.352
	third metatarsophalangeal joint	3.52		0.497
	fourth metatarsophalangeal joint	2.88		0.417

Backgrounds for unguligrades with pads are colored gray.

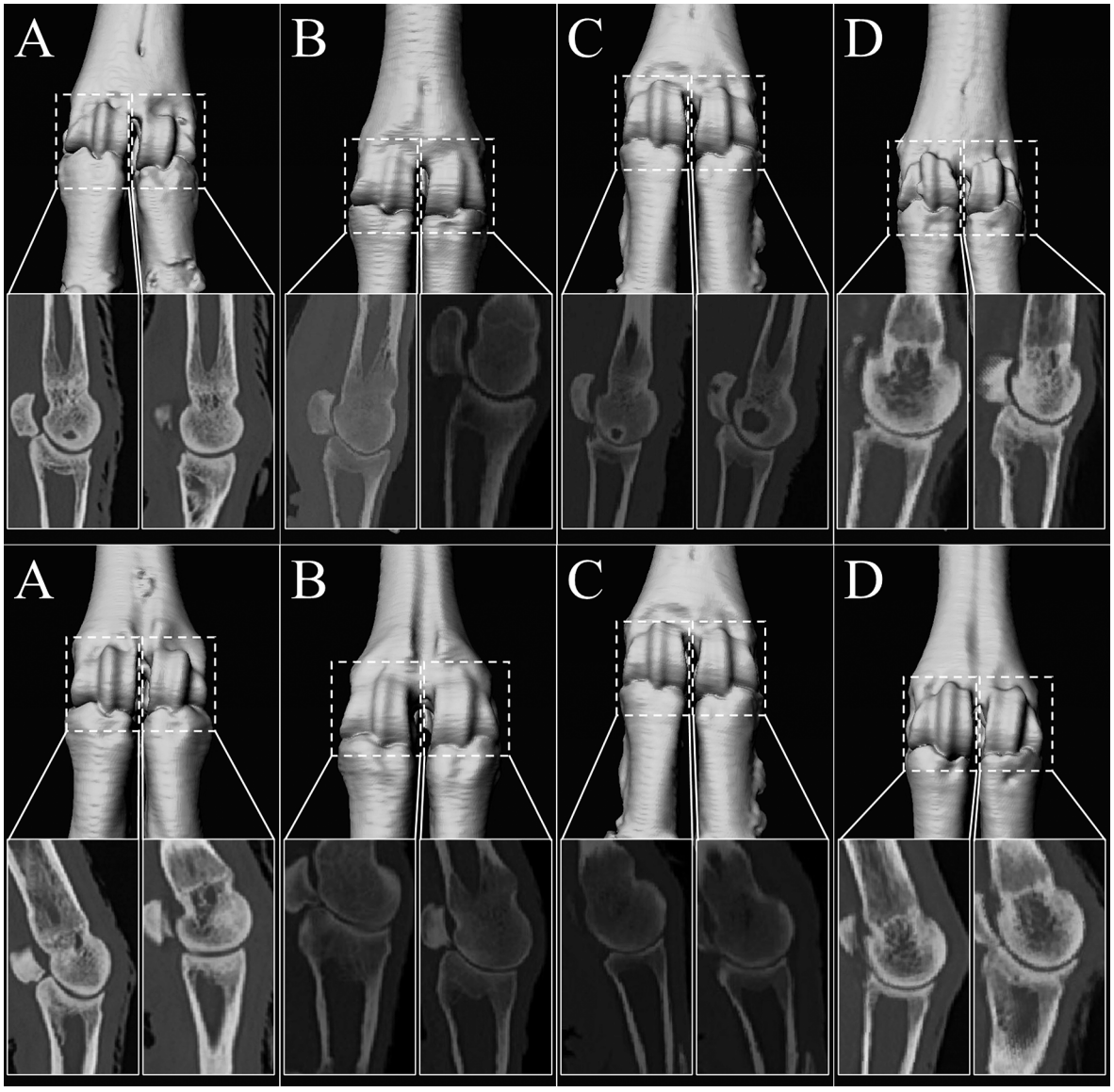

Fig. 2. Left extremities in unguligrades in dorsal view. The metapodiophalangeal joints are enclosed by dashed line squares, and the solid line squares show sagittal cross sections of the metapodiophalangeal joints. No distinct gap was observed at the metapodiophalangeal joints since the articular facets of the proximal phalanges were curved to follow the articular facets of the metapodials. A) *C. falconeri*. B) *O. leucoryx*. C) *O. canadensis*. D) *P. nayaur*. Upper: forelimb, Lower: hindlimb.

of the second and third fingers were 2.8° and 2.2°, respectively, and those of the proximal phalanges of the third and fourth fingers were 1.4° (Table 5). Among unguligrades with pads, *L. glama* showed large angle changes, whereas the other four species showed similar or lower values than the unguligrade *O. leucoryx* (Tables 4 and 5).

In the hindlimb, the difference in angle between the opening and closing states of unguligrade species *C. falconeri*, *O. leucoryx*, *O. canadensis*, and *P. nayaur* was 6.9°, 1.3°, 3.4° and 4.1°, respectively (Table 6). *Camelus bactrianus*, *C. dromedarius*, and *L. glama* changed the angle of the proximal phalanges by 3.2°, 2.3°, and 5.5° between opening and closing, respectively (Table 6). In *C. simum* and *R. unicornis*, the angle changes of the proximal phalanges of the second and third fingers were 2.4° and 2.6°, respectively, and those of the proximal phalanges of the third and fourth fingers were 3.2° and 2.5° (Table 7). Compared to the forelimbs, the angle changes in the hindlimbs of unguligrades were unaltered or smaller, whereas the angle changes in the hindlimbs of unguligrades with pads were unaltered or larger. However, even though the angle changes in the hindlimbs of

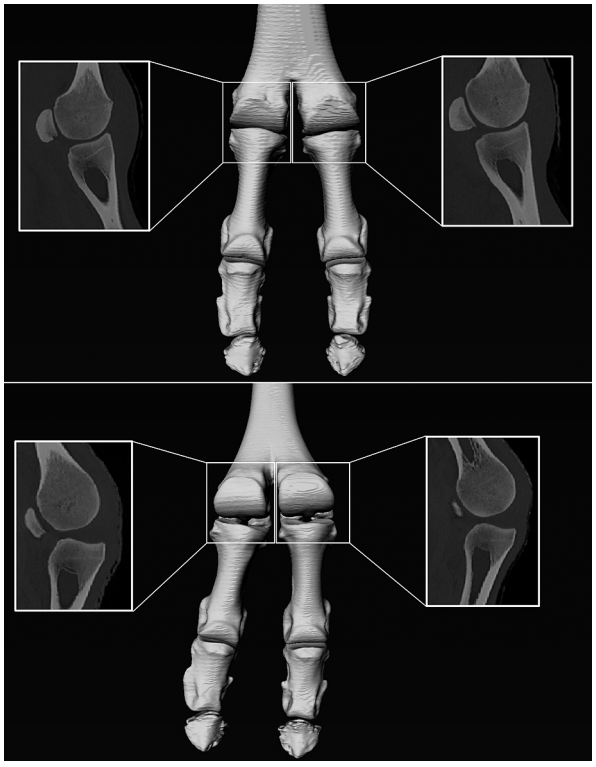

Fig. 3. Left extremities and metapodiophalangeal joints in *C. bactrianus* in dorsal view. The metapodiophalangeal joints are enclosed by thin line squares, and the thick line squares show sagittal cross sections of the metapodiophalangeal joints. The articular facets of the proximal phalanges were straight, and large gaps were observed between the metapodials and the proximal phalanges. Upper: forelimb, Lower: hindlimb.

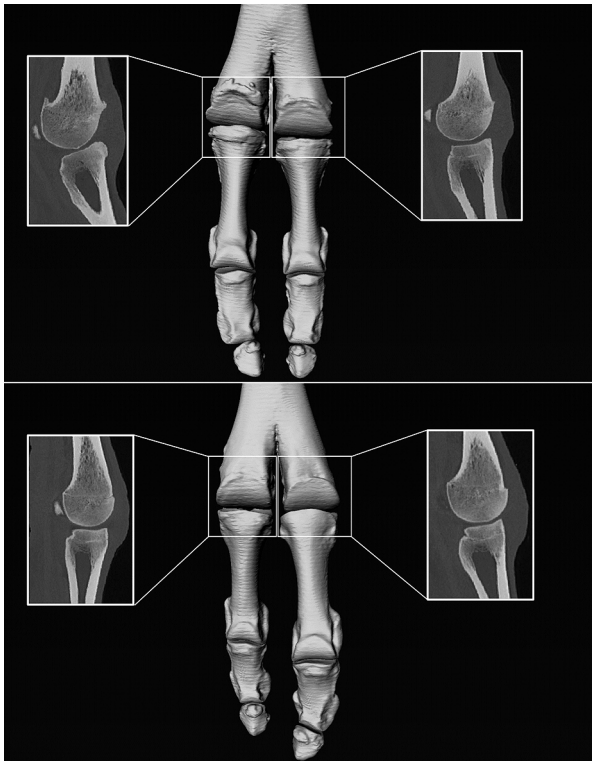

Fig. 4. Left extremities and metapodiophalangeal joints in *C. dromedarius* in dorsal view. The metapodiophalangeal joints are enclosed by thin line squares, and the thick line squares show sagittal cross sections of the metapodiophalangeal joints. The articular facets of the proximal phalanges were straight, and large gaps were observed between the metapodials and the proximal phalanges. Upper: forelimb, Lower: hindlimb.

Table 4. Angle data in the metacarpophalangeal joints of Artiodactyla

Species	State	Angle (degree)	Angle change (degree)
C. falconeri	Closing	7.4	
	Opening	14.9	7.5
O. leucoryx	Closing	6.2	
	Opening	8.4	2.2
O. canadensis	Closing	3.5	
	Opening	9.9	6.3
P. nayaur	Closing	6.3	
	Opening	12.6	6.2
C. bactrianus	Closing	11.4	
	Opening	12.1	0.7
C. dromedarius	Closing	12.2	
	Opening	14.9	2.7
L. glama	Closing	4.6	
	Opening	10.0	5.4

Backgrounds for unguligrades with pads are colored gray.

Table 5. Angle data in the metacarpophalangeal joints of Rhinocerotidae

Species	State	Position	Angle (degree)	Angle change (degree)
C. simum	Closing	2nd–3rd proximal phalanges	24.9	
		3rd–4th proximal phalanges	28.5	
	Opening	2nd–3rd proximal phalanges	27.7	2.8
		3rd–4th proximal phalanges	29.9	1.4
R. unicornis	Closing	2nd–3rd proximal phalanges	22.8	
		3rd–4th proximal phalanges	23.4	
	Opening	2nd–3rd proximal phalanges	25.0	2.2
		3rd–4th proximal phalanges	24.8	1.4

Backgrounds for unguligrades with pads are colored gray.

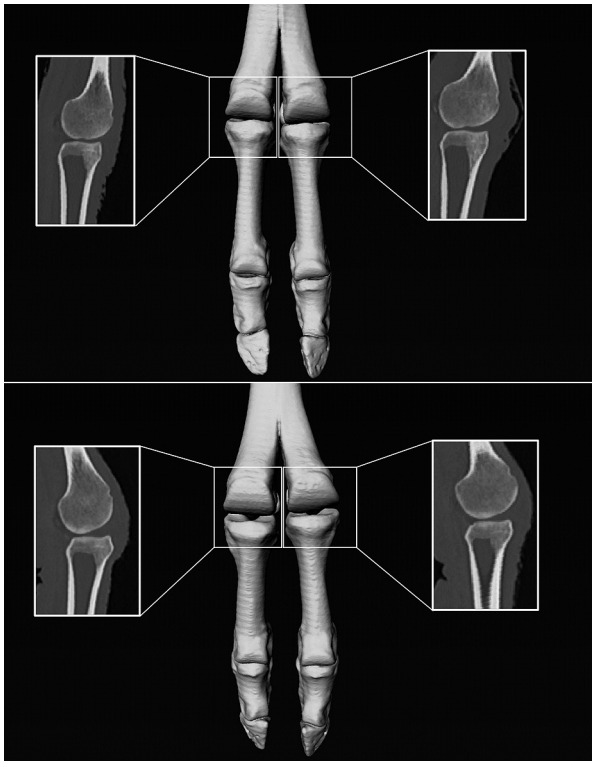

Fig. 5. Left extremities and metapodiophalangeal joints in *L. glama* in dorsal view. The metapodiophalangeal joints are enclosed by thin line squares, and the thick line squares show sagittal cross sections of the metapodiophalangeal joints. The articular facets of the proximal phalanges were straight, and large gaps were observed between the metapodials and the proximal phalanges. Upper: forelimb, Lower: hindlimb.

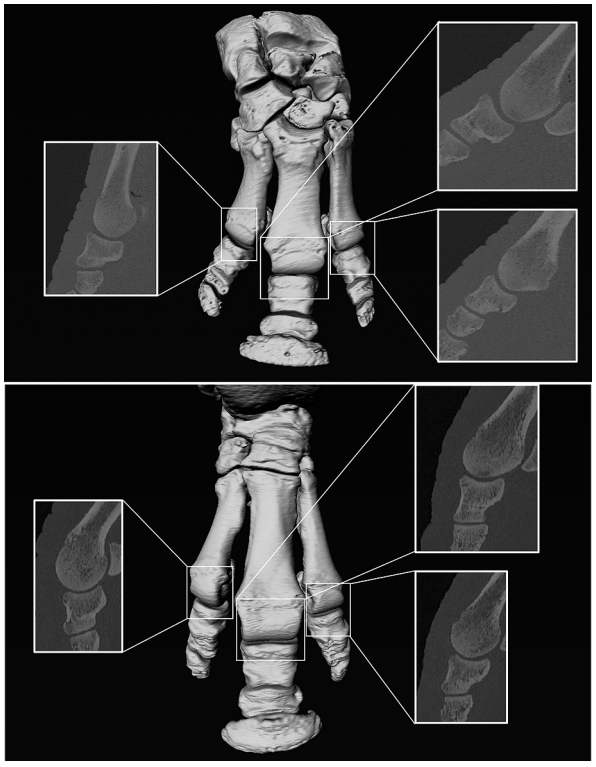

Fig. 6. Left extremities and metapodiophalangeal joints in *C. simum* in dorsal view. The metapodiophalangeal joints are enclosed by thin line squares, and the thick line squares show sagittal cross sections of the metapodiophalangeal joints. The articular facets of the proximal phalanges were straight, and large gaps were observed between the metapodials and the proximal phalanges. Upper: forelimb, Lower: hindlimb.

Table 6. Angle data in the metatarsophalangeal joints of Artiodactyla

Species	State	Angle (degree)	Angle change (degree)
C. falconeri	Closing	6.2	
	Opening	13.1	6.9
O. leucoryx	Closing	1.7	
	Opening	3.0	1.3
O. canadensis	Closing	3.6	
	Opening	6.9	3.4
P. nayaur	Closing	9.4	
	Opening	13.6	4.1
C. bactrianus	Closing	8.9	
	Opening	12.1	3.2
C. dromedarius	Closing	7.2	
	Opening	9.5	2.3
L. glama	Closing	6.9	
	Opening	12.4	5.5

Backgrounds for unguligrades with pads are colored gray.

Table 7. Angle data in the metatarsophalangeal joints of Rhinocerotidae

Species	State	Position	Angle (degree)	Angle change (degree)
C. simum	Closing	2nd–3rd proximal phalanges	20.2	
		3rd–4th proximal phalanges	21.3	
	Opening	2nd–3rd proximal phalanges	22.6	2.4
		3rd–4th proximal phalanges	24.5	3.2
R. unicornis	Closing	2nd–3rd proximal phalanges	19.7	
		3rd–4th proximal phalanges	21.8	
	Opening	2nd–3rd proximal phalanges	22.3	2.6
		3rd–4th proximal phalanges	24.3	2.5

Backgrounds for unguligrades with pads are colored gray.

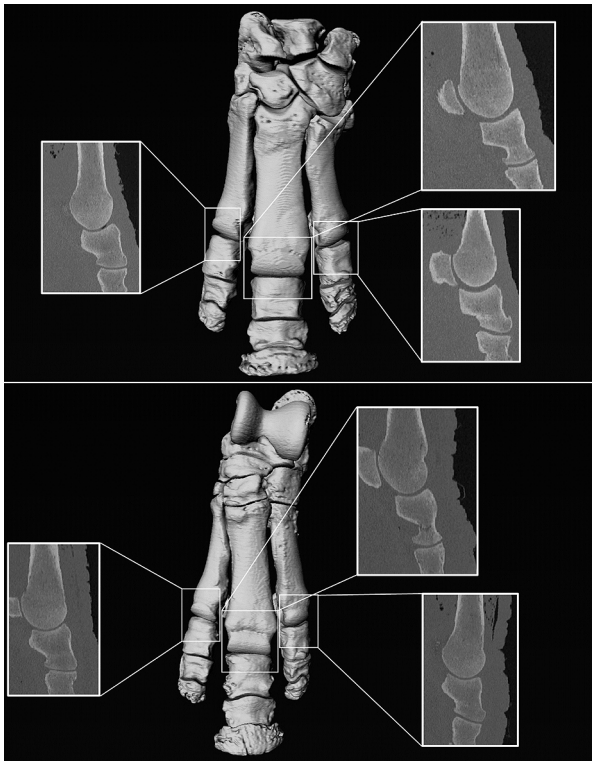

Fig. 7. Left extremities and metapodiophalangeal joints in *R. unicornis* in dorsal view. The metapodiophalangeal joints are enclosed by thin line squares, and the thick line squares show sagittal cross sections of the metapodiophalangeal joints. The articular facets of the proximal phalanges were straight, and large gaps were observed between the metapodials and the proximal phalanges. Upper: forelimb, Lower: hindlimb.

unguligrades with pads was larger, it was not larger than the angle changes in unguligrades.

Observation of the extremities of the necropsy specimens revealed that the pads and fingers were connected in *C. dromedarius* and *R. unicornis*, making it difficult to move each digit independently. In contrast, the pads are divided into separate fingers in *H. amphibius* and *T. indicus* (Fig. 8 and Supplementary Fig. S1).

Discussion

The distal ends of the metapodials of unguligrades possess a trochlear keel (Janis and Scott 1987; Clifford 2010). The metapodial keels prevent the metapodiophalangeal joints from spreading by fitting into the groove in the proximal facets of the proximal phalanges (Cope 1889; Wortman 1893). 3D images of extremities showed that metapodiophalangeal joints of unguligrades with pads were not equipped with tightly connected structures (Figs. 3–7); thus, the skeletal morphology did not have the ability to limit finger spreading as in unguligrades. However, the angle changes in the proximal phalanges of unguligrades with pads were similar to that of *O. leucoryx* and smaller than that of *C. falconeri*, *O. canadensis*, and *P. nayaur*. The mountainous species such as *C. falconeri*, *O. canadensis*, and *P. nayaur* exhibit large angle changes in the proximal phalanges, whereas *O. leucoryx*, a species that appears in plains, shows smaller angle changes than most bovids (Takeda et al. 2023). The fact that the angle changes of unguligrades with pads with large gaps in the metapodiophalangeal joints were similar to that of *O. leucoryx*, which shows smaller angle changes among the bovids, suggests that factors other than skeletal morphology may prevent digits from spreading in the unguligrades with pads. The phalanges of unguligrades with pads are arranged to rest on pads (Smuts and Bezuidenhout 1987; von Houwald 2001). Pads absorb shock and disperse foot pressure (Panagiotopoulou et al. 2012, 2016, 2019; Clemente et al. 2020). However, although the pads are elastic, they do not change shape significantly. This suggests that the angle changes of the proximal phalanges were smaller in the unguligrades with pads since their digits are connected by the pads. The bovids, unguligrades, adapted to diverse terrains by changing the angle of digit opening and closing (Takeda et al. 2023). However, unguligrades with pads are hard to change the angle of digit opening and closing, making it more difficult for them to inhabit diverse terrains compared to unguligrades. Among the extant species of unguligrades with pads, the tapir and the hippopotamus live in wetlands, whereas the rhinoceros include both plain-dwelling and wetland-dwelling species (Wilson and Mittermeier 2011). Of the Camelidae, the dromedary camel and bactrian camel are distributed in the desert (Wilson and Mittermeier 2011). The Camelidae llama, guanaco, alpaca, and vicuña, which live in mountainous areas, possess smaller pads than the dromedary camel and bactrian camel (Wilson and Mittermeier 2011; König et al. 2015). Accordingly, only a few unguligrades with pads inhabit mountainous areas, while most live in plains or wetlands. In contrast, unguligrades include several species adapted to steep mountainous terrain (Wilson and Mittermeier 2011). The distribution of the extant species also suggests that the unguligrades tend to be more adaptable to diverse terrains than the unguligrades with pads.

Among unguligrades with pads, the proximal phalanges of *L. glama* spread wide in the opening state compared to the closing state (Tables 4 and 5). Llamas possess

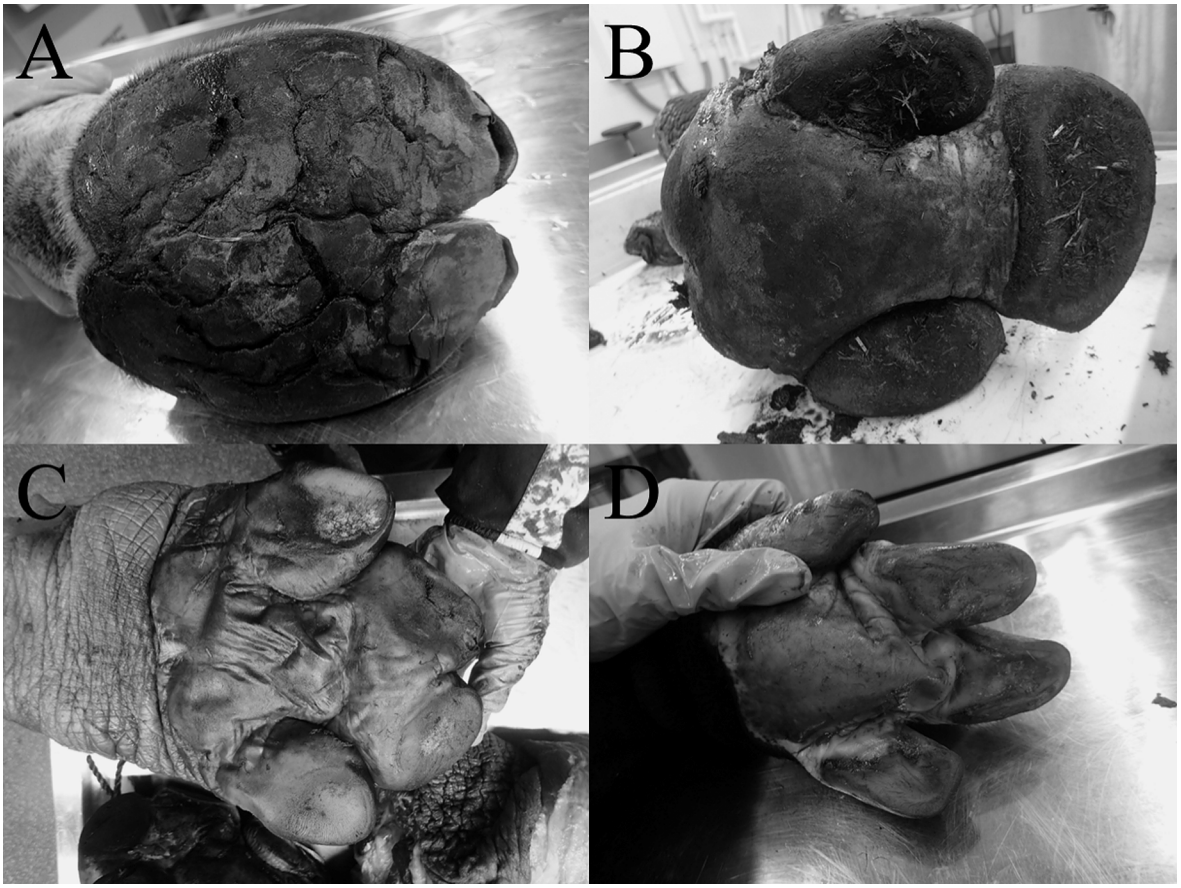

Fig. 8. Extremities of forelimb viewed from palmar aspect. A) Left foot of *C. dromedarius*. B) Left foot of *R. unicornis*. C) Right foot of *H. amphibius*. D) Right foot of *T. indicus*.

relatively reduced pads compared to dromedary camels and bactrian camels (König et al. 2015). This suggests that the llama's digits are less restricted by pads to open and close than those of other unguligrades with pads, allowing for more proximal phalanges movement. The dromedary camels and bactrian camels are distributed in deserts, whereas llamas live in mountains (Wilson and Mittermeier 2011). Bovids living in mountains can move better on unstable substrates due to their increased digit mobility (Scott 1985; Rozzi and Palombo 2013a, 2013b; Takeda et al. 2023). Llamas, like bovids that inhabit mountainous areas, may use the spreading of their fingers to stabilize themselves on the rocky mountainous terrain. However, even in *L. glama*, which do not possess tightly connected metapodiophalangeal joints (Fig. 5), the angle changes were not larger than in unguligrades such as *C. falconeri* (Tables 4 and 6). This suggests that unguligrades, either with or without pads, need to develop the ability to restrain the digits from spreading.

Hippopotamuses and tapirs, which are unguligrades with pads, move their medial and lateral digits during the opening and closing states for their semi-aquatic walking (Endo et al. 2019). Figure 8 and Supplementary Fig. S1 showed the extremities of *C. dromedarius*, *R. unicornis*, *H. amphibius*, and *T. indicus* viewed from palmar or plantar aspect. In rhinoceros and camel, the pads connect the fingers, whereas in hippopotamus and tapir, the pads are divided into separate fingers (Fig. 8 and Supplementary Fig. S1). This suggests that hippopotamuses and tapirs may spread their digits more widely than rhinoceroses and camels. Whether hippopotamuses and tapirs open their digits similarly to the bovids that inhabit mountainous terrains should be noticed. The white rhinoceroses are plain-dwelling, whereas the Indian rhinoceroses are semi-aquatic (Wilson and Mittermeier 2011). Indian rhinoceroses were expected to spread their digits widely, as did hippopotamuses and tapirs. However, the results of this study showed no clear difference in angle changes between *C. simum* and *R. unicornis* (Tables 5 and 7). If large-sized species like rhinoceroses were equipped with

highly mobile digits, the risk of tearing between the digits would increase. The evolution of larger size is associated with foot posture transitions in mammals (Kubo et al. 2019). In addition, fat pads in camels contribute to adaptation to large size rather than adaptation to the desert (Clemente et al. 2020). Therefore, it is suggested that unguligrades with pads exhibit phylogenetically and morphologically determined body size, and that large unguligrades with pads may limit finger mobility to reduce the risk of tearing between the digits.

The pads on the extremities of unguligrades with pads contribute to supporting their large body size by distributing foot pressure (Panagiotopoulou et al. 2012, 2016, 2019; Clemente et al. 2020). However, the pads restrict digit mobility, possibly confining unguligrades with pads to living only in certain types of terrains. In contrast, unguligrade that are not equipped with pads on their extremities are able to have greater digit mobility. Consequently, they have adapted to a more diverse range of terrains than unguligrades with pads.

Supplementary data

Supplementary data are available at *Mammal Study* online.
Supplementary Fig. S1. Extremities of hindlimb viewed from plantar aspect. A) Left foot of *C. dromedarius*. B) Left foot of *R. unicornis*. C) Right foot of *H. amphibius*. D) Right foot of *T. indicus*.

Acknowledgments: We wish to express our gratitude to Izu Shaboten Zoo, Kanazawa Zoological Gardens, Tobu zoo, Yokohama Zoological Gardens ZOORASIA, and Yumemi Zoo for their support in the dissection of the rare carcass. This study was financially supported by JSPS KAKENHI Grant Numbers 21K00985, 22H00013 and 23KK0009.

References

Clemente, C. J., Dick, T. J., Glen, C. L. and Panagiotopoulou, O. 2020. Biomechanical insights into the role of foot pads during locomotion in camelid species. Scientific Reports 10: 1–12.

Clifford, A. B. 2010. The evolution of the unguligrade manus in artiodactyls. Journal of Vertebrate Paleontology 30: 1827–1839.

Cope, E. D. 1889. The Artiodactyla (continued). The American Naturalist 23: 111–136.

Endo, H., Yoshida, M., Nguyen, T. S., Akiba, Y., Takeda, M. and Kudo, K. 2019. Three-dimensional CT examination of the forefoot and hindfoot of the hippopotamus and tapir during a semiaquatic walking. Anatomia, Histologia, Embryologia 48: 3–11.

Gregory, W. K. 1912. Notes on the principles of quadrupedal locomotion and on the mechanism of the limbs in hoofed animals. Annals of the New York Academy of Sciences 22: 267–294.

Howell, A. B. 1944. Speed in Animals, their Specialization for Running and Leaping. University of Chicago Press, Chicago, 270 pp.

Janis, C. M. and Scott, K. M. 1987. The interrelationship of higher ruminant families: with special emphasis on the member of the Cervoidea. American Museum Novitates 2893: 1–85.

Janis, C. M. and Wilhelm, P. B. 1993. Were there mammalian pursuit predators in the Tertiary? Dances with wolf avatars. Journal of Mammalian Evolution 1: 103–125.

König, H. E., Skewes, O., Helmreich, M. and Böck, P. 2015. Macroscopic and histological investigation of guanaco footpads (*Lama guanicoe*, Müller 1776). Journal of Morphology 276: 331–341.

Kubo, T., Sakamoto, M., Meade, A. and Venditti, C. 2019. Transitions between foot postures are associated with elevated rates of body size evolution in mammals. Proceedings of the National Academy of Sciences 116: 2618–2623.

Panagiotopoulou, O., Pataky, T. C., Day, M., Hensman, M. C., Hensman, S., Hutchinson, J. R. and Clemente, C. J. 2016. Foot pressure distributions during walking in African elephants (*Loxodonta africana*). Royal Society Open Science 3: 160203. DOI: 10.1098/rsos.160203.

Panagiotopoulou, O., Pataky, T. C., Hill, Z. and Hutchinson, J. R. 2012. Statistical parametric mapping of the regional distribution and ontogenetic scaling of foot pressures during walking in Asian elephants (*Elephas maximus*). Journal of Experimental Biology 215: 1584–1593.

Panagiotopoulou, O., Pataky, T. C. and Hutchinson, J. R. 2019. Foot pressure distribution in White Rhinoceroses (*Ceratotherium simum*) during walking. PeerJ 7: e6881. DOI: 10.7717/peerj.6881.

Rozzi, R. and Palombo, M. R. 2013a. The morphology of femur as palaeohabitat predictor in insular bovids. Bollettino della Societa Paleontologica Italiana 52: 177–186.

Rozzi, R. and Palombo, M. R. 2013b. Do methods for predicting paleohabitats apply for mountain and insular fossil bovids? Integrative Zoology 8: 244–259.

Scott, K. M. 1985. Allometric trends and locomotor adaptations in the Bovidae. Bulletin of the American Museum of Natural History 179: 197–288.

Smuts, M. M. S. and Bezuidenhout, A. J. 1987. Anatomy of the Dromedary. Oxford University Press, Oxford, 230 pp.

Takeda, S., Oshida, T., Motokawa, M., Kawada, S. and Endo, H. 2023. Morphology of metapodiophalangeal joints and mobility of finger and toe in bovids. Mammal Study 48: 145–157.

Thomason, J. J. 1986. The functional morphology of the manus in the tridactyl equids *Merychippus* and *Mesohippus*: paleontological inferences from neontological models. Journal of Vertebrate Paleontology 6: 143–161.

von Houwald, F. 2001. Foot Problems in Indian Rhinoceroses (*Rhinoceros unicornis*) in Zoological Gardens: Macroscopic and Microscopic Anatomy, Pathology, and Evaluation of the Causes. Ph. D. Dissertation, University of Zurich, Zurich, 104 pp.

Wilson, D. E. and Mittermeier, R. A. 2011. Handbook of the Mammals of the World, Volume 2: Hoofed Mammals. Lynx Ediciones, Barcelona, 886 pp.

Wortman, J. L. 1893. A new theory of the mechanical evolution of the metapodial keels of Diplarthra. The American Naturalist 27: 421–434.

Received 5 March 2024. Accepted 23 August 2024.
Editor was Mugino Kubo.